High Rotation Number Effect on Heat Transfer in a Triangular Channel With 45 deg, Inverted 45 deg, and 90 deg Ribs

Yao-Hsien Liu
Department of Mechanical Engineering,
National Chiao Tung University,
Hsinchu 30010, Taiwan
e-mail: yhliu@mail.nctu.edu.tw

Michael Huh
Department of Mechanical Engineering,
University of Texas at Tyler,
Tyler, TX 75799
e-mail: mhuh@uttyler.edu

Je-Chin Han
Department of Mechanical Engineering,
Turbine Heat Transfer Laboratory,
Texas A&M University,
College Station, TX 77843-3123
e-mail: jc-han@tamu.edu

Hee-Koo Moon
Solar Turbines Inc.,
San Diego, CA 92186

Heat transfer and pressure drop have been experimentally investigated in an equilateral triangular channel ($D_h = 1.83$ cm), which can be used to simulate the internal cooling passage near the leading edge of a gas turbine blade. Three different rib configurations (45 deg, inverted 45 deg, and 90 deg) were tested at four different Reynolds numbers (10,000–40,000), each with five different rotational speeds (0–400 rpm). The rib pitch-to-height (P/e) ratio is 8 and the height-to-hydraulic diameter (e/D_h) ratio is 0.087 for every rib configuration. The rotation number and buoyancy parameter achieved in this study were 0–0.58 and 0–2.3, respectively. Both the rotation number and buoyancy parameter have been correlated with predict the rotational heat transfer in the ribbed equilateral triangular channel. For the stationary condition, staggered 45 deg angled ribs show the highest heat transfer enhancement. However, staggered 45 deg angled ribs and 90 deg ribs have the higher comparable heat transfer enhancement at rotating condition near the blade leading edge region. [DOI: 10.1115/1.4000986]

Keywords: heat transfer, turbulence promoter, triangular channel, high rotation number

1 Introduction

The leading edge of the gas turbine blade is critical due to high heat load. Internal cooling technique can be applied by circulating compressed air through the multipass cooling cavities inside blade structure. Cooling channels with different geometry are applicable to different regions of the turbine blade, as shown in Fig. 1. It shows that the triangular-shaped channel and wedge-shaped channel can be applied to the leading edge and trailing edge of the blade, respectively. Internal cooling is influenced by the channel aspect ratio, turbulence promoter configurations, rotational and flow parameters. *Gas Turbine Heat Transfer and Cooling Technology* [1] provides in-depth information about the state of the art cooling techniques.

Early internal cooling research began with square or rectangular channels [2–5]; however, they are commonly used in the middle portion of the turbine blade. A triangular-shaped cooling channel is a more realistic design to fit the profile of the blade leading edge. Studies focused on triangular channels at stationary condition provide a good starting point to understand the heat transfer in leading edge cavities. The heat transfer and pressure drop measurements inside the triangular channel were in good agreement with the correlations developed for turbulent tube flow using the hydraulic diameter of the triangular duct as the tube diameter [6]. Metzger and Vedula [7] experimentally measured heat transfer in triangular channels with angled ribs on two walls. They studied three different rib angles and three different sets of rib orientations. For all the test configurations, 60 deg angled ribs produce higher heat transfer than 30 deg angled ribs, and $P/e=7.5$ rib spacing yield the best thermal performance (TP). Zhang et al. [8] tested heat transfer in a triangular duct with full and partial ribbed walls. They found that the heat transfer coefficients and friction factors in triangular ducts with partial ribbed walls (90 deg or 45 deg ribs) were 10% higher than those with fully ribbed walls. Haasenritter and Weigand [9] performed a numerical study of heat transfer in a rib-roughened triangular channel. The results show good agreement with the experimental data from Ref. [7]. Ahn and Son [10] studied heat transfer and pressure drop in a rib-roughened equilateral triangular channel with $P/e=4$, 8, and 16. They concluded that the $P/e=8$ had the best thermal performance with the Reynolds number from 10,000 to 70,000. Amro et al. [11] also experimentally investigated heat transfer inside a ribbed triangular channel. Considering the local as well as overall heat transfer enhancement and the friction factor, they concluded that 45 deg inclined ribs were the optimum. Not only the triangular channels have been studied, the trapezoidal channels with the similar shape also provide valuable information. Taslim et al. [12] measured heat transfer coefficients and friction factor in the trapezoidal channel by liquid crystal technique. They found that the roughening of the partition walls enhances the heat transfer coefficients on those walls but, more importantly, enhances heat transfer coefficients on the primary walls considerably. Takeishi et al. [13] performed an experimental and analytical study on the heat transfer and pressure drop in a triangular cooling channel with the gap between sidewall and ribs. The conclusion was optimizing the length of the gap enables the enhancement of the heat transfer around the trailing edge and to assure mean heat transfer in the while of the cooling flow passage.

In the actual turbine blade, the rotor blade is rotating and the effect of rotation in the cooling channels should be considered. The secondary flow induced by rotation has great impact in the smooth channel as well as in the ribbed channel. Dutta et al. [14] studied heat transfer in a two-pass rotating triangular duct with the rotation number from 0 to 0.22. They studied two channel orientations to the direction of rotation. For the radially outward flow in the first pass, the Nusselt number ratios increase with rotation on the trailing wall and reduce on the leading wall. Lee et al. [15] measured the heat transfer and pressure drop in a rotating equilateral triangular channel with three different rib arrangements: 45 deg, 90 deg, and 135 deg. The highest rotation number was 0.1 at

Contributed by the Heat Transfer Division of ASME for publication in the JOURNAL OF HEAT TRANSFER. Manuscript received August 8, 2009; final manuscript received November 1, 2009; published online April 29, 2010. Assoc. Editor: Frank Cunha.

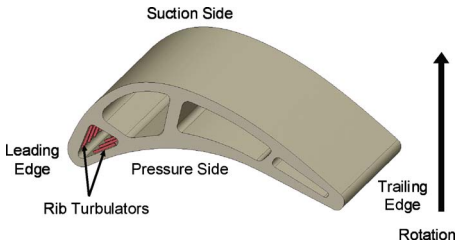

Fig. 1 Internal gas turbine blade cooling passage

Reynolds number of 10,000. They showed that the thermal performance for 45 deg and 135 deg angled ribs is very similar and both are higher than the 90 deg ribs.

The effect of rotation needs to be tested under high rotation numbers in order to simulate the actual engine condition. Currently, most of the data available in the high rotation number domain is limited to square or rectangular channel. Wagner et al. [16] performed heat transfer measurements inside a smooth square channel with radial outward flow in the first pass. The rotation number ranged from 0.00 to 0.48 in their studies. Wagner et al. [17] continued to investigate the heat transfer inside the second and third passage of the smooth square channel. The results from Refs. [16,17] showed that both the rotation number and density ratio (DR) caused large changes in heat transfer for radially outward flow but relatively small changes for radially inward flow. Johnson et al. [18] performed heat transfer measurements in a rotating square channel with ribs skewed to the flow and compared the results from the smooth channel. They found that heat transfer with skewed ribs is less sensitive to the buoyancy than the heat transfer inside the smooth channel or normal ribbed channel. Zhou et al. [19] investigated the heat transfer in a 4:1 channel under high rotation numbers from 0 to 0.6. They concluded that there is a critical rotation number where the trend of the heat transfer enhancement begins to reverse. Liou et al. [20] investigated the heat transfer in a rectangular channel ($AR=1:2$) with 45 deg angled ribs under high rotation numbers from 0 to 2. They found that the 45 deg staggered ribs generated overall heat transfer enhancement of 1.6–4.3 times higher than the Dittus–Boelter correlation in the Reynolds number range of 5000–15,000. Liu et al. [21] studied the heat transfer in a two-pass rectangular ($AR=1:4$) channel under high rotation numbers from 0 to 0.67. They found that the buoyancy parameter can be used to quantify the effect of rotation. Wright et al. [22] conducted heat transfer measurements in a wedge-shaped trailing edge channels under high rotation numbers from 0 to 1.0. It showed that the nondimensional rotation number and buoyancy parameter not only can be used in the rectangular channel but also valid in this wedge-shaped channel.

Liu et al. [23] investigated the heat transfer inside an equilateral triangular channel with a smooth and 45 deg angled ribbed surface. The objective is to do an extended research from the previous study [23], and the performance of different rib configurations inside this triangular cooling channel is compared. The details are as follows.

1. Investigate heat transfer distribution in the equilateral triangular ribbed channel under stationary and rotating conditions. Since the thermal load varies near the leading edge of the turbine blade, each surface of the channel is divided into two regions to provide local heat transfer distribution.
2. Study heat transfer and pressure drop inside the triangular channel with three different rib configurations (45 deg, inverted 45 deg, and 90 deg). The highest rotation number is 0.58 under the applicable Reynolds number of 10,000.
3. The Reynolds numbers, the rotational speeds, and the coolant-to-wall density ratios were varied in order to obtain a thorough understanding of the rotation number and buoyancy parameter effects. Correlation functions have been generated to predict the heat transfer enhancement.

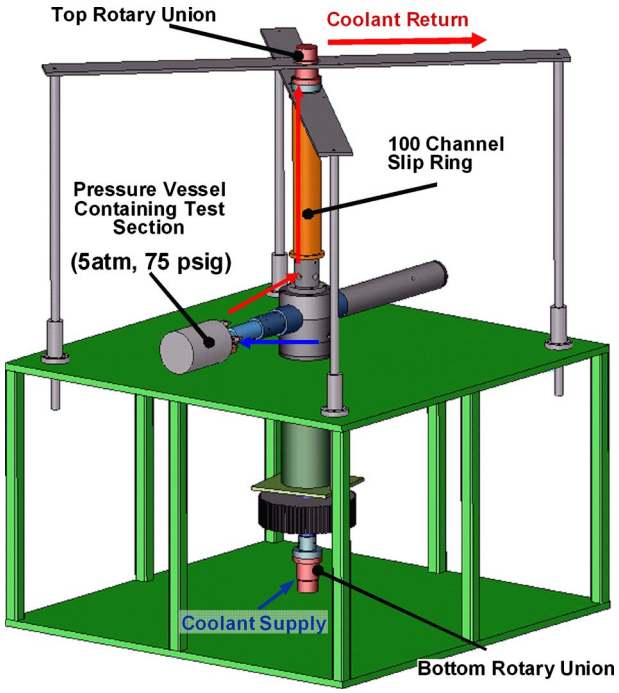

Fig. 2 Rotating facility

2 Experimental Setup

2.1 Rotating Facility. The study of heat transfer inside rotating cooling channel is performed in a rotating facility as shown in Fig. 2. Coolant air enters from the bottom of the rig through a rotary union into the hollow shaft. The air continues to travel through the hub to a rubber hose and goes into the pressure vessel containing the test section. After the air passes through the heated test section, the air goes through another rubber hose to the copper tubing inside slip ring. The copper tubing connects to another rotary union at the top of the slip ring. A needle valve is attached to the pipe to adjust the pressure of the flow loop. With the air pressurized at 5 times atmospheric pressure, the rotation number reached in this triangular channel is 0–0.58. A motor is used to drive the shaft with a frequency controller to control the rotational speeds from 0 rpm to 400 rpm. A 100 channel slip-ring is used as an interface to transfer the data reading from the rotating test section to the data acquisition system.

2.2 Triangular Channel With Ribs. The equilateral triangular test section used is shown in Fig. 3(*a*). The coolant air comes from a 1.27 cm diameter pipe into the inlet part. Two mesh screens were placed at the inlet part to help spread the flow. The thickness of the inlet part is 3.81 cm with the $L_e/D_h=2.09$. The inlet part has a slot with the same cross section as the triangular test section and is fully attached to the test section parts. The coolant flow goes radially outward into the test section and discharges into the cavity of the pressure vessel then back to the flow loop. Two pressure taps were placed at the inlet and another two pressure taps were placed at the outlet to measure the pressure drop across the test section.

The triangular test section consists of three parts: leading, trailing, and inner walls as shown in Fig. 3(*b*). These three pieces are made of Garolite and the thickness of each piece is 2.54 cm. The size of each copper plate is 1.35×1.11 cm^2 with the thickness of 0.476 cm. The copper plates on the leading and trailing surfaces were in staggered arrangement. The gaps between the copper plates were filled with silicon as an insulation layer. A blind hole

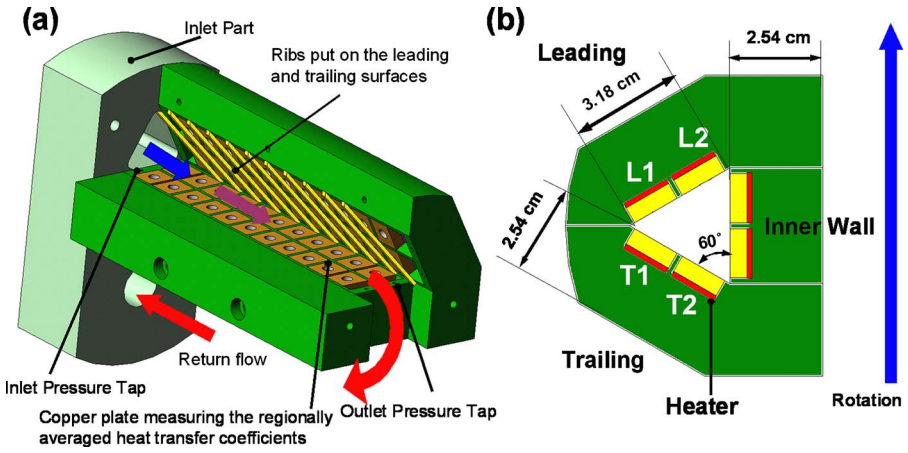

Fig. 3 (*a*) **Details of the triangular test section and** (*b*) **cross-sectional view of the test section**

was drilled in each copper plate and a thermocouple was glued in each hole with epoxy. Electric resistant heaters were placed beneath the copper plates in each row. The channel orientation was 90 deg to the direction of rotation.

In the current study, the ribs were glued on the leading and trailing surfaces with super glue. The square ribs were made of brass with the cross section of 1.59×1.59 mm^2. Three different rib configurations were tested with the same P/e ratio of 8 and e/D_h ratio of 0.087. Figure 4 shows these three rib configurations (45 deg angled, inverted 45 deg angled, and 90 deg orthogonal). Due to the staggered arrangement of the copper plates, the ribs on the leading surface and trailing surface were also staggered. In order to eliminate the conduction effects caused by the continuous ribs across different surfaces, insulation was filled between the gaps as shown in Fig. 4.

3 Data Reduction

3.1 Heat Transfer Measurement. As described with the experimental setup, regionally averaged heat transfer coefficients were measured in the current study. The heat transfer coefficients can be determined from Newton's Law of Cooling as demonstrated in Eq. (1).

$$h = \frac{\dot{Q}_{\text{net}}}{A(T_{w,x} - T_{b,x})} = \frac{\dot{Q}_{\text{in}} - \dot{Q}_{\text{loss}}}{A(T_{w,x} - T_{b,x})} \tag{1}$$

The net rate of heat transfer is determined from the difference of the power supplied to each resistance heater and the heat lost from the test section. The heat loss is determined by inserting the insulation material into the channel to eliminate natural convection. Power is supplied by the heaters, and the power required to reach a series of given temperatures is recorded. The power supplied to the heaters during this calibration is equivalent to the actual experimental heat loss. Separate heat loss calibrations are required for each rotational speed.

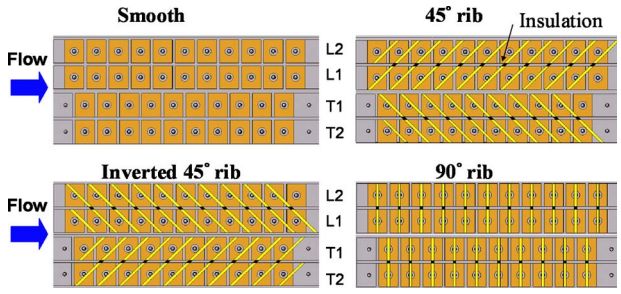

Fig. 4 Rib configurations of the current study

The regional wall temperature ($T_{w,x}$) is measured using the thermocouple fixed in each copper plate. The coolant bulk temperature at a specific location ($T_{b,x}$) in the channel is determined by the linear interpolation between the measured inlet and outlet temperatures. The Nusselt number is used to quantify the heat transfer enhancement (or declination) due to either the specific channel geometry or rotation. The Nusselt number ratio (Nu/Nu_o) is used to show the heat transfer enhancement relative to fully developed, turbulent heat transfer in a circular tube (Dittus–Boelter–McAdams correlation, Nu_o). Equation (2) shows this Nusselt number ratio.

$$\frac{\text{Nu}}{\text{Nu}_o} = \left(\frac{hD_h}{k}\right)\left(\frac{1}{0.023\ \text{Re}^{0.8}\ \text{Pr}^{0.4}}\right) \tag{2}$$

3.2 Friction Factor Ratio and Thermal Performance. The friction factor can be calculated from the pressure drop between the inlet and the outlet of the channel as shown in Eq. (3).

$$f = (\Delta P)/4\left(\frac{L}{D_h}\right)\frac{1}{2}\rho V^2 \tag{3}$$

The pressure difference (ΔP) is taken as the difference between the inlet pressure and outlet pressure readings. The frictional losses can then be calculated by dividing the fiction factor by the turbulent friction factor in a smooth tube as given by the Blasius equation. With the friction factor in a smooth tube defined as f_o, the friction factor ratio can be expressed in terms of the measured friction factor, and the smooth channel friction factor, as shown in Eq. (4).

$$f/f_0 = f/0.079\ \text{Re}^{-0.25} \tag{4}$$

Based on the heat transfer enhancement (Nu/Nu_o) and the frictional loss penalty (f/f_o), the TP for a given rib configuration can be calculated. Equation (6) shows the thermal performance based on the constant pumping power condition.

$$\text{TP} = (\text{Nu}/\text{Nu}_0)/(f/f_0)^{1/3} \tag{5}$$

3.3 Uncertainty Analysis. The experimental uncertainty for the presented results was calculated using the method developed and published by Kline and McClintock [24]. Air properties were taken based on the mean bulk air temperature. The uncertainty for the temperature measurement in the triangular channel is 0.3 °C. The uncertainty of the Nusselt number ratio is approximately

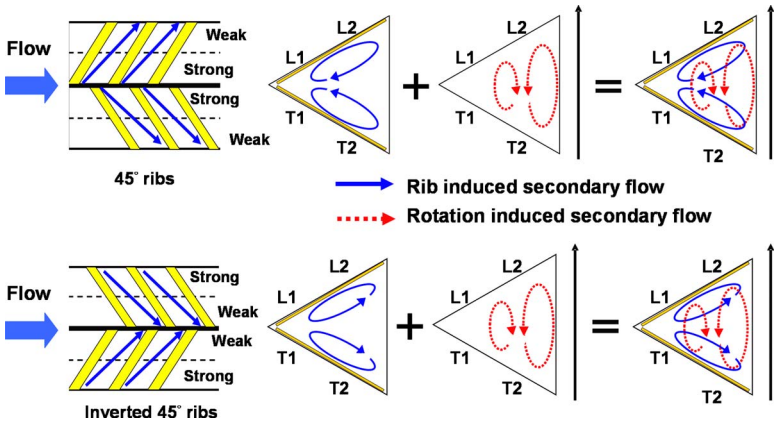

Fig. 5 Conceptual view of the rib and rotation induced secondary flow in a rotating ribbed channel

4.9% for the highest Reynolds number (Re=40,000). For the lowest Reynolds number (Re=10,000), the maximum uncertainty is approximately 9.8%. The maximum uncertainty for the pressure measurement is 9.7% at Re=10,000 and drops to 4.7% at Re =40,000.

4 Results and Discussion

4.1 Heat Transfer in the Stationary Channel. In the current experimental setup, it is in the developing flow condition because of the short entrance length (L_e/D_h=2.09). Heat transfer is enhanced and the baseline data comparisons were shown in the previous work [23]. Heat transfer is influenced by the channel geometry and the flow condition inside the stationary channel. Angled ribs induce secondary flow along the rib orientations as speculated in Fig. 5 and heat transfer distribution is altered. 45 deg angled ribs induced secondary flow goes from the rib leading region (L1 and T1) toward the rib trailing region (L2 and T2). The strength of this secondary flow decreases along the rib orientation and it tends to impinge on the rib leading region (L1 and T1). Therefore, the heat transfer enhancement is higher in the rib leading region (L1 and T1) than the rib trailing region (L2 and T2). For inverted 45 deg angled ribs, the secondary flow structure is reversed as the rib is inverted.

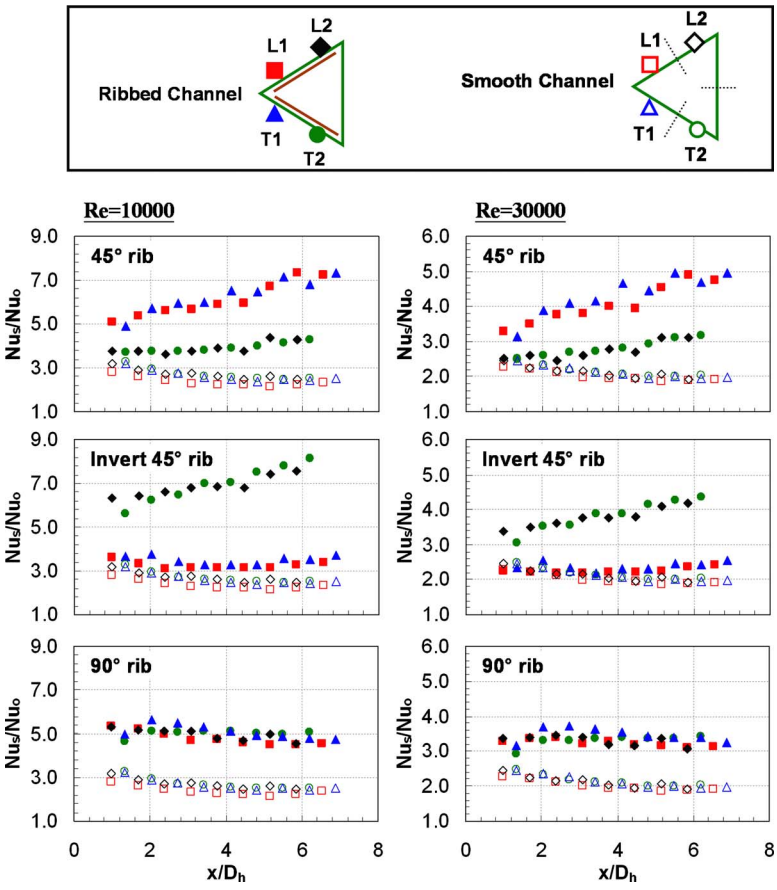

Fig. 6 Nusselt number ratio distribution in the stationary channel

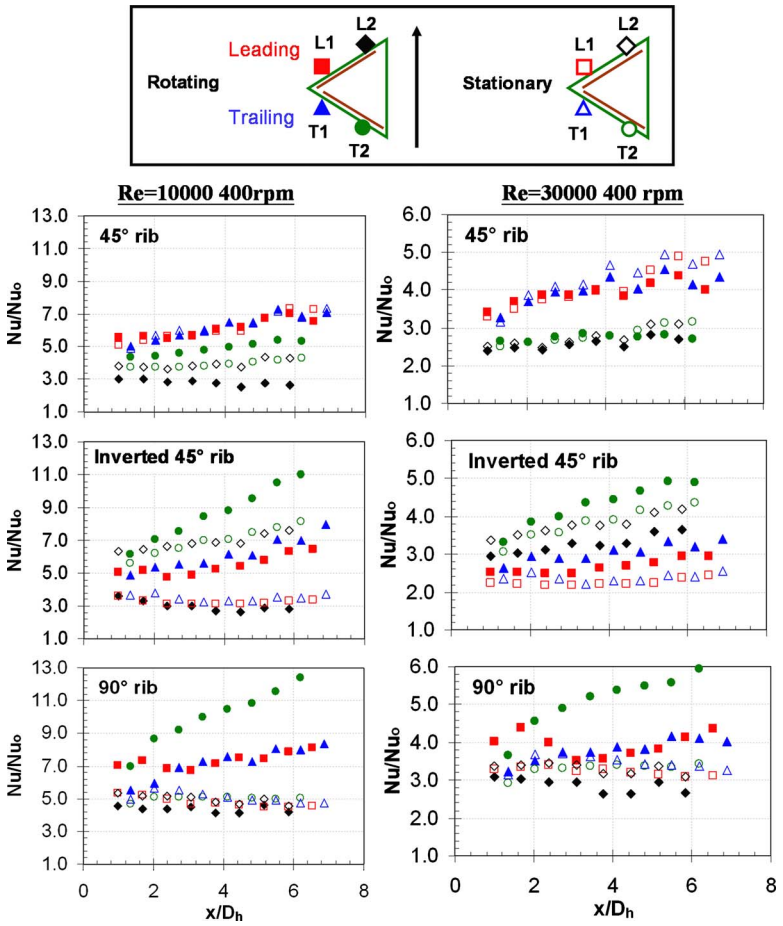

Fig. 7 Nusselt number ratio distribution in the rotating channel

Figure 6 shows the Nusselt number ratios (Nu/Nu_o) in the stationary channel with smooth case and ribbed cases. Two different Reynolds numbers of 10000 and 30000 are reported for each case. For the 45 deg ribbed channel, the heat transfer enhancement in the rib leading region (L1 and T1) is higher than the rib trailing region (L2 and T2). This is a good design for high heat load portion near the blade leading region. The angled rib induced secondary flow grows in strength as the flow goes over several additional ribs and the heat transfer is increased gradually along the streamwise direction. The Nusselt number ratio increases along the streamwise direction from 5.0 to 7.4 in L1 and T1 regions at Re=10,000. It increases along the streamwise direction from 3.8 to 4.3 in L2 and T2 regions at Re=10,000. The entire ribbed leading and trailing surfaces both have higher heat transfer than the smooth cases. However, as the Reynolds number increases from 10,000 to 30,000, the heat transfer enhancement by the ribs decreases. For the inverted 45 deg angled ribs, the rib induced secondary flow is reversed compared with the 45 deg angled ribs. Therefore, the higher heat transfer occurs on L2 and T2 surfaces while the lower heat transfer occurs on L1 and T1 surfaces. It shows the reversed heat transfer trend as compared with the 45 deg angled rib. Heat transfer is only slighted altered by the ribs on L1 and T1 surfaces and is smaller than L2 and T2 region. For 90 deg orthogonal ribs, heat transfer is influenced mainly due to ribs tripping the flow and the flow reattachment. There is no rib induced secondary flow along the rib orientation and heat transfer is more uniformly altered across the entire channel. The Nusselt number ratios (Nu/Nu_o) on these four regions are very similar and decrease gradually along the streamwise direction as shown in Fig. 6. At Reynolds number of 10,000, Nusselt number ratio on the leading surface (L1 and L2) decreases from 5.4 to 4.5 along the streamwise direction. The Nusselt number ratio is about 1.7 times higher than the smooth case at Re =10,000 and 1.5 times higher than the smooth surface at Re =30,000.

4.2 Heat Transfer in the Rotating Channel. Before the detailed discussion of the rotating results, it is necessary to describe the effect of rotation inside cooling channels. Two counter rotating vortices are generated due to Coriolis force during rotation. For the radially outward flow, rotation increases heat transfer on the trailing surface while decreases heat transfer on the leading surface. The structure of these two counter rotating vortices varies depending on the channel geometry and the channel orientation. Figure 5 shows this secondary flow pattern in the current study, which also involves the formation of the two counter rotating vortices. In a ribbed channel, the rib induced secondary flow interacts with the rotating induced secondary flow and the heat transfer behavior is affected by the combined effects from both as shown in Fig. 5. The effect of rotation is small and does not have significant impact on heat transfer on the rib leading surface (L1 and T1) because rib induced secondary flow dominates. While near the rib trailing surface (L2 and T2), the wide space allows the rotation induced secondary flow to develop freely and the effect of rotation is more obvious. With the ribs put on the leading and trailing surfaces, the Nusselt number ratio distributions in both the stationary and rotating channels (400 rpm) are shown in Fig. 7.

For 45 deg angled ribs, it has high heat transfer near L1 and T1 regions and the heat transfer improvement due to rotation is limited. While on the rib trailing region (L2 and T2), the effect of rotation is more obvious and enhances heat transfer on the trailing

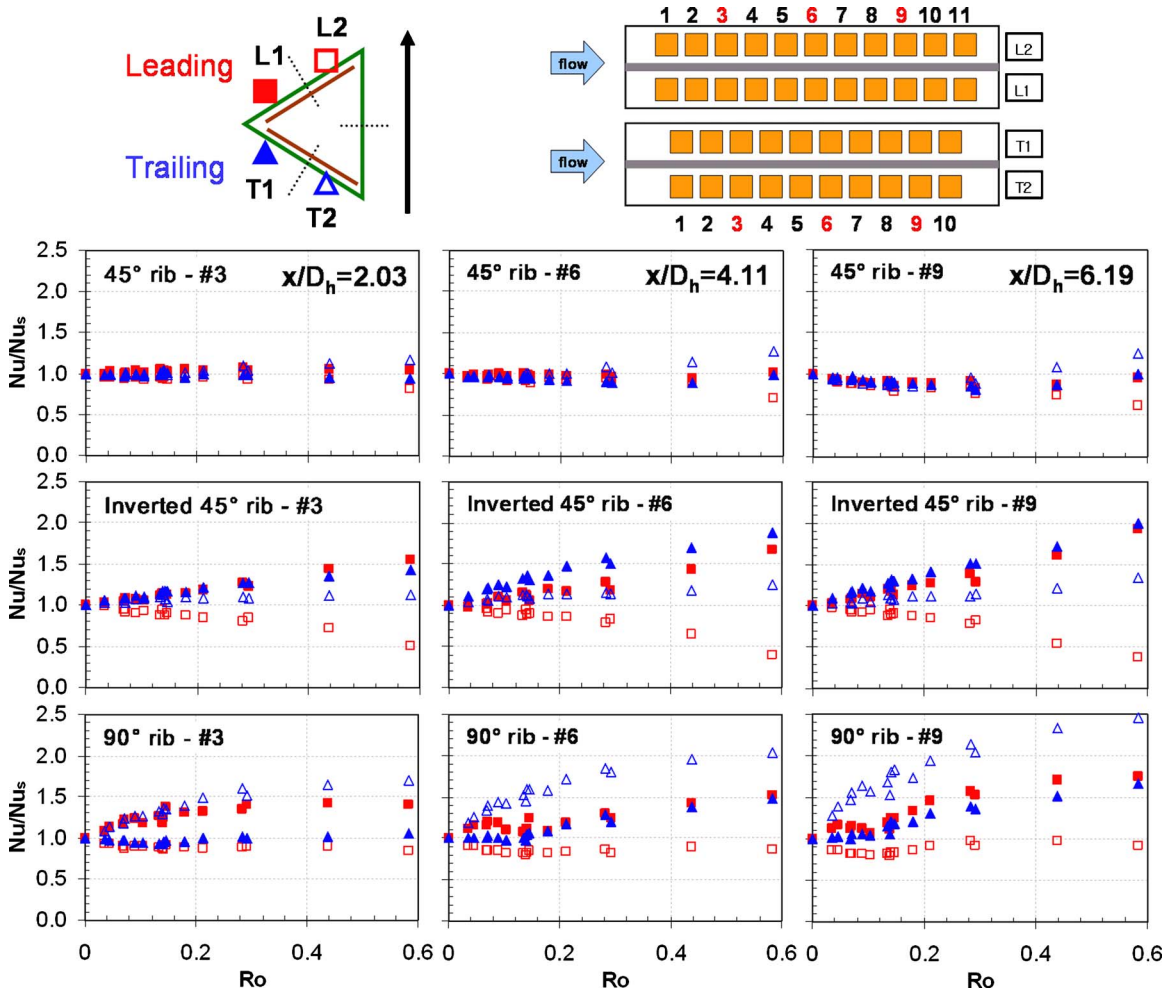

Fig. 8 Effect of rotation number on three different regions

surface while decreases heat transfer on the leading surface. On the L2 region, the rib induced secondary flow opposes the rotation induced secondary flow and produces lowest heat transfer.

It can be expected that the direction of rib induced secondary flow is reversed while the rotation induced secondary flow remains the same for the inverted 45 deg angled ribs. On the T2 surface, both the rib and rotation induced secondary flows interact together to enhance heat transfer and the highest heat transfer occurs due to the combined effects. Nusselt number ratio ($\mathrm{Nu}/\mathrm{Nu}_o$) increases from 6.0 to 11.0 along the streamwise direction at Re=10,000. Heat transfer on the T1 surface is slightly higher than the L1 surface due to effect of rotation but both higher than the stationary case. Therefore, the L1 surface has the lowest heat transfer at Re=30,000. However, the L2 surface has the lowest heat transfer at Re=10,000 due to stronger effect of rotation (higher rotation number).

Heat transfer is the highest on the T2 surface and the lowest on the L2 surface for 90 deg orthogonal ribs. The rotating heat transfer is mainly affected by the effect of rotation because there is no secondary flow along the rib orientation. Nusselt number ratio increases dramatically from 7.0 to 13.0 on the T2 surface along the streamwise direction at Re=10,000; however, it increases slightly on L1 and T1 surfaces from 7.0 to 8.4. Nu ratio on the L2 surface is the lowest and remains the same level along the streamwise direction. As the Reynolds number increases, the Nusselt number ratio ($\mathrm{Nu}/\mathrm{Nu}_o$) decreases and the difference between stationary and rotating results also decreases. Thus, the effect of rotation is reduced.

4.3 Rotation Number Effects. Rotation number is a ratio of Coriolis force to the bulk flow inertia force. By varying the rotational speed (Coriolis force) and the Reynolds number (flow inertia force), the contribution from these two factors should yield the same results. The rotation number is defined in Eq. (6).

$$\mathrm{Ro} = \frac{\Omega D_h}{V} \tag{6}$$

This nondimensional parameter is widely used to quantify the effect of rotation in the industry and academia. Heat transfer enhancement due to effect of rotation is represented by the ratio of the rotational Nusselt number to the stationary Nusselt number ($\mathrm{Nu}/\mathrm{Nu}_s$). Figure 8 shows this heat transfer enhancement ($\mathrm{Nu}/\mathrm{Nu}_s$) with Reynolds number from 10,000 to 40,000 and rotational speed from 0 rpm to 400 rpm. Three different regions (3, 6, and 9) in the streamwise direction (x/D_h=2.03, 4.11, and 6.19, respectively) are chosen to study the rotation number effects.

The Nusselt number ratios ($\mathrm{Nu}/\mathrm{Nu}_s$) with rotation number for 45 deg angled ribs are presented from region 3 to region 9. The heat transfer enhancements ($\mathrm{Nu}/\mathrm{Nu}_s$) on L1 and T1 surfaces are very similar, which indicate the effect of rotation is small and the rib induced secondary flow dominates. In region 3, Nusselt number ratio decreases gradually from 1.0 to 0.8 with the rotation number on the L2 surface and gradually increases from 1.0 to 1.2 with the rotation number on the T2 surface. When the flow moves downstream to regions 6 and 9, the difference between L2 and T2

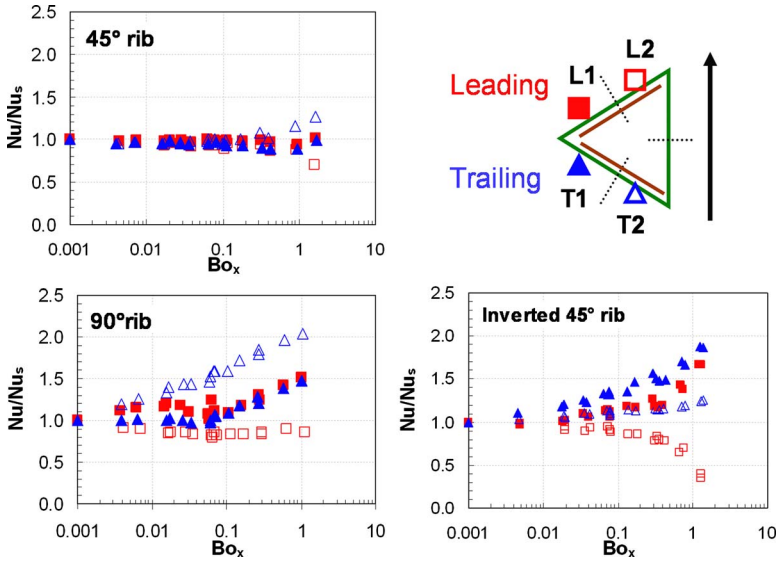

Fig. 9 Effect of Buoyancy Parameter on Nusselt number ratios at x/D_h =4.11

surfaces becomes larger than region 3. For 45 deg angled ribs, heat transfer enhancement/degradation due to effect of rotation is smallest among all the cases.

For inverted 45 deg angled ribs, heat transfer enhancements on all the surfaces increase with Ro except for the L2 surface. On L1 and T1 surfaces, Nusselt number ratio (Nu/Nu_s) increases from 1.0 to 1.5 in region 3 and from 1.0 to 2.0 in region 9 with rotation number. Heat transfer enhancement due to rotation is smaller near the entrance of the channel because of entrance effect. The Nusselt number ratio (Nu/Nu_s) on L1 and T1 surfaces is high due to low Nusselt number at stationary condition (Nu_s). On the T2 surface, heat transfer enhancement increases slightly with rotation number. Nu/Nu_s increases up to 1.1 in region 3 and 1.35 in region 9. Heat transfer enhancement due to rotation is smaller compared with L1 and T1 surfaces. Heat transfer on T2 surface is already high at stationary condition and thus enhancement due to rotation is limited. On the L2 surface, Nu/Nu_s decreases gradually down to 0.5 in region 3 and 0.4 in regions 6 and 9 with rotation number.

For 90 deg orthogonal ribs, heat transfer enhancement is the highest on the T2 surface and the lowest on the L2 surface. On the T2 surface, Nu/Nu_s increases with rotation number up to 1.7 in region 3 and 2.5 in region 9. For the L2 surface, heat transfer enhancement maintains the same level of 0.8 as rotation number increases and the effect of rotation in this region is minimal. The L2 surface has the lowest Nusselt number ratio due to rotation for all the ribbed cases. In region 3, Nu/Nu_s maintains the same level with rotation number on the T1 surface but increases with the rotation number on L1 surfaces. It is noted that Nu/Nu_s on the T1 surface is lower than the L1 surface due to staggered ribs near the entrance under rotating condition in region 3. In regions 6 and 9, Nu/Nu_s increases gradually with rotation number for L1 and T1 surfaces. For 90 deg orthogonal ribs, there is no significant heat transfer declination as rotation number increases; therefore, overall heat transfer gradually increases with rotation.

4.4 Buoyancy Parameter Effects. The buoyancy parameter is also a widely used nondimensional parameter to quantify the effect of rotation inside the gas turbine blade. The buoyancy force due to centrifugal force and temperature difference is important because of the high rotating speed and large temperature difference in the actual engines. The buoyancy parameter considers all factors affecting the effect of rotation: the density ratio (temperature difference), the rotation number, and the rotating radius. It is shown in Eq. (7).

$$\mathrm{Bo}_x = \left(\frac{\Delta\rho}{\rho}\right)_x (\mathrm{Ro})^2 \frac{R_x}{D_h} = \frac{T_{w,x} - T_{b,x}}{T_{f,x}} (\mathrm{Ro})^2 \frac{R_x}{D_h} \tag{7}$$

The local film temperature is defined as the average of the local wall temperature and the local bulk temperature as shown in Eq. (8).

$$T_{f,x} = (T_{w,x} + T_{b,x})/2 \tag{8}$$

In the current study, the region near the middle portion of the channel (x/D_h=4.11) is chosen to study the effect of buoyancy parameter on Nusselt number ratios (Nu/Nu_s). All the cases were tested at the coolant-to-wall DR of 0.11.

Figure 9 shows the Nusselt number ratio (Nu/Nu_s) for 45 deg, inverted 45 deg, and 90 deg ribs. For the 45 deg angled ribs, Nusselt number ratio (Nu/Nu_s) remains the same level on L1 and T1 surfaces as the buoyancy parameter increases. Heat transfer is enhanced slightly on the T2 surface while declined slightly on the L2 surface. Nusselt number ratio (Nu/Nu_s) increases up to about 1.3 in the T2 region while decreases down to about 0.7 in the L2 region at the maximum buoyancy parameter of 1.9. For 90 deg orthogonal ribs, Nusselt number ratio (Nu/Nu_s) maintains the same level as buoyancy parameter increases on the L2 surface. Nu/Nu_s increases with buoyancy parameter on L1, T1, and T2 surfaces. It is noted that there is no significant heat transfer degradation for all the regions. High heat transfer due to rotation can be expected at high buoyancy parameter for the 90 deg orthogonal ribs.

Two additional coolant-to-wall DRs of 0.13 and 0.15 were tested specifically for inverted 45 deg rib case to study the density ratio effects. Total of three different density ratios (0.11, 0.13, and 0.15) were plotted. On the leading surface, L1 increases with buoyancy parameter while L2 decreases with buoyancy parameter. For the entire trailing surface, Nusselt number ratio (Nu/Nu_s) increases with the buoyancy parameter as shown in the figure. The heat transfer enhancement on the T1 surface is higher than the T2 region. The data with different density ratios fit nicely into the curve. It shows that the density ratio, Reynolds number, and rotational speed can be varied independently but the results still can be correlated into a single curve by buoyancy parameter.

4.5 Average Heat Transfer. The Nusselt number ratios (Nu/Nu_o) were averaged along the streamwise direction for every surface (L1, T1, L2, and T2), as shown in Fig. 10. Results are

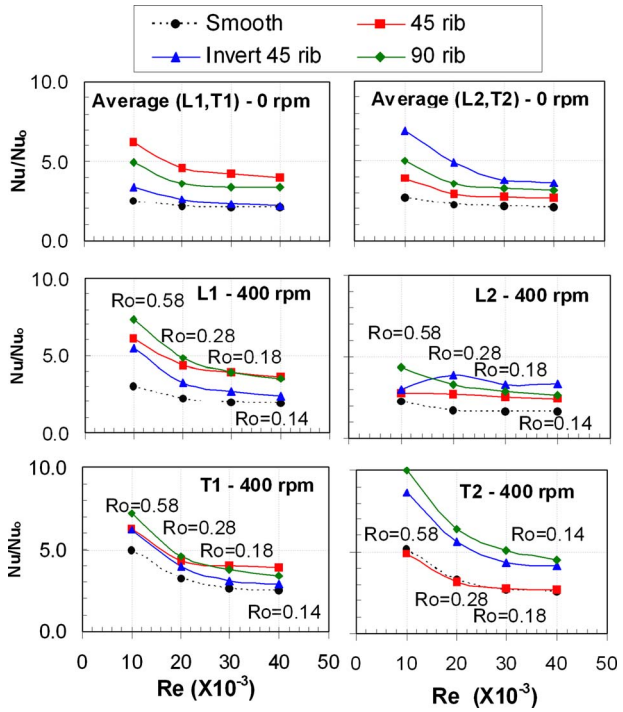

Fig. 10 Average heat transfer results at stationary and rotating conditions

compared between stationary and the highest rotational speed (400 rpm) to investigate the effect of rotation. The two regions (L1 and T1) can be used to represent the blade leading edge region of the gas turbine where high thermal load exists. At stationary condition, 45 deg rib has the highest heat transfer while the inverted 45 deg rib has the lowest heat transfer for average of the L1 and T1 surfaces. From this figure, we can conclude that although heat transfer for 45 deg rib is the highest at stationary case; heat transfer of 90 deg rib is comparable with 45 deg rib at rotating condition. The heat transfer enhancement level increases as Reynolds number decreases (rotation number increases). Inverted 45 deg rib has the highest heat transfer for the average of the L2 and T2 surfaces at stationary condition, as shown in Fig. 10. For rotating condition, inverted 45 deg and 90 deg rib have the comparable heat transfer enhancement on the L2 and T2 surfaces. It is

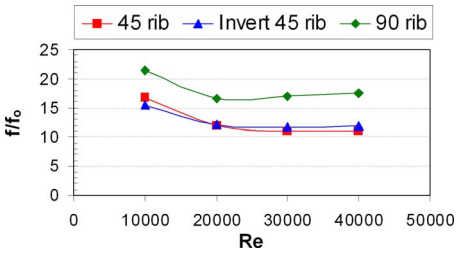

Fig. 11 Friction factor ratio of different rib configurations

noticed that the Nu ratio for 45 deg rib is the lowest on these surfaces and is very close to the smooth case on the T2 surface.

4.6 Friction Factor Ratio and Thermal Performance. One way to evaluate the performance of different ribs is to calculate the thermal performance for each rib configuration. In the current study, the pressure drop is measured for all the cases at stationary condition. The friction factor ratios are shown in Fig. 11. 90 deg rib has the higher friction factor ratio than the 45 deg and inverted 45 deg angled ribs.

Thermal performance near the leading edge of the turbine blade (L1 and T1 surfaces) and the total average at stationary condition are presented in Fig. 12. For the L1 and T1 surfaces, 45 deg rib has the highest thermal performance while inverted 45 deg rib has the lowest thermal performance at stationary condition. The total average thermal performance is based on the average Nusselt number ratios (Nu/Nu_o) from the leading and trailing surfaces. Angled ribs usually have higher thermal performance than the orthogonal ribs due to smaller pressure drop. Results show that 45 deg rib still has the best thermal performance and 90 deg rib has the worst thermal performance at stationary condition.

4.7 Correlations for Heat Transfer Enhancement. The average Nusselt number ratios (Nu/Nu_s) on the leading and trailing surfaces are plotted in Fig. 13. Each data point is the average of 18 points over the entire leading or trailing surfaces. The results are plotted with the rotation number and the average buoyancy parameter. The well-correlated curve shows that rotation number and buoyancy parameter can be used to predict the heat transfer enhancement inside this triangular channel with smooth and ribbed surfaces. It is well correlated for all the three rib cases by a power function with the maximum discrepancy within ±6.8%. The constants for the correlation functions are shown in Table 1.

The results for 45 deg angled ribbed and smooth cases were

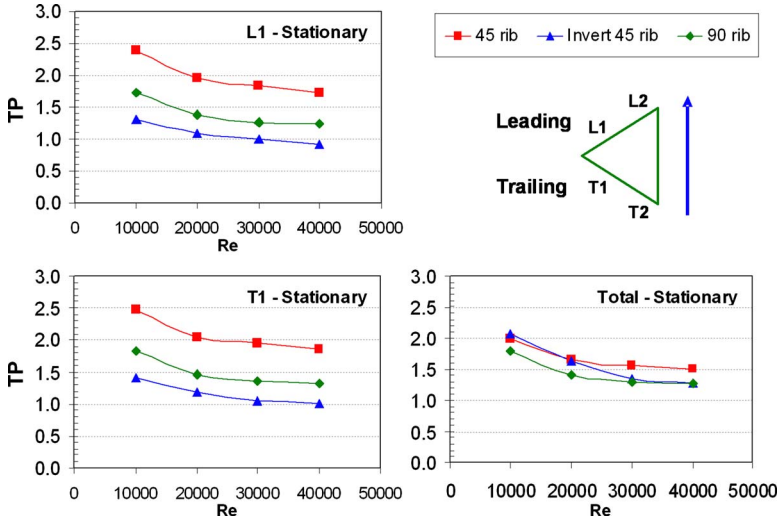

Fig. 12 Thermal performance comparison of L1, T1, and total average

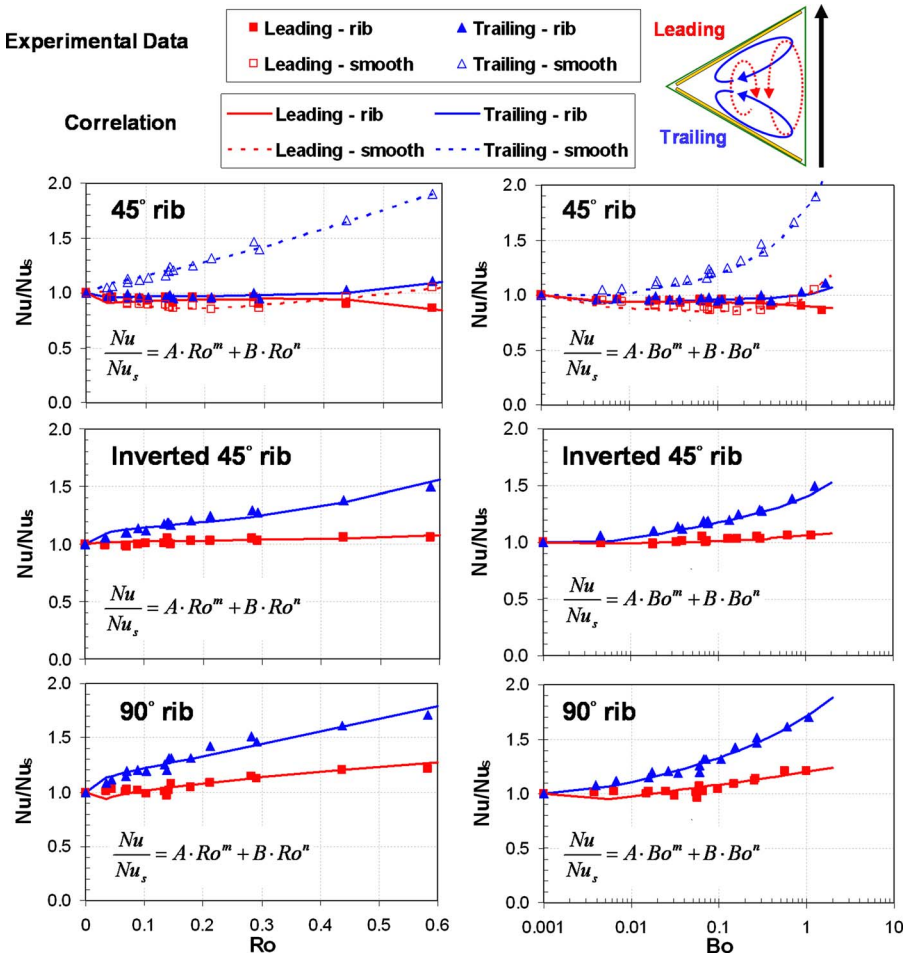

Fig. 13 Correlations for heat transfer enhancement

plotted together for comparison. The heat transfer enhancement due to rotation for the smooth case is higher than the 45 deg ribbed case. The heat transfer enhancement/degradation for the smooth case occurs at a lower rotation number and buoyancy parameter than the ribbed case. For the ribbed case, the Nu/Nu_s values on the leading and trailing surfaces are very close when rotation number is smaller than 0.3. After that, the Nusselt number ratios on the leading and trailing surfaces begin to diverge. Figure 13 also shows the Nu/Nu_s with the average buoyancy parameters. The trends are very similar to the plots with the rotation number. For the inverted 45 deg angled ribs, the average Nusselt number ratio (Nu/Nu_s) increases with rotation number and buoyancy parameter on both the leading and trailing surfaces. The Nu ratio (Nu/Nu_s) increases up to 1.5 on the trailing surface while only increases up to 1.1 on the leading surface as rotation number and buoyancy parameter increases. For 90 deg ribs, both the leading and trailing surface increase with rotation number and buoyancy parameter. Trailing surface has higher heat transfer enhancement than the leading surface. It shows that the heat transfer enhancement due to rotation for 90 deg rib is the highest among all the rib cases.

5 Conclusion

Heat transfer and pressure drop have been measured in a rotating equilateral triangular channel to model the cooling channel near the leading edge of the gas turbine blade. The results on the leading and trailing surfaces of the channel were reported. The

Table 1 Correlation coefficients for the heat transfer enhancement

	Ro				Bo			
	A	*m*	*B*	*n*	*A*	*m*	*B*	*n*
Leading—smooth	0.97	0.02	−10.00	7.50	0.80	−0.02	0.18	1.10
Trailing—smooth	0.50	−0.20	0.80	0.95	1.10	0.02	−0.20	0.25
Leading—45 deg rib	1.19	0.04	1.60	1.45	1.21	0.04	0.55	0.80
Trailing—45 deg rib	0.99	0.01	1.90	5.50	0.98	0.01	0.02	2.00
Leading—inverted 45 deg	1.05	0.01	0.50	5.50	0.90	−0.01	0.16	0.25
Trailing—inverted 45 deg	1.25	0.04	1.20	2.50	1.30	0.05	0.10	0.80
Leading—90 deg rib	1.10	0.05	0.35	1.05	1.41	0.06	−0.21	0.12
Trailing—90 deg rib	1.22	0.03	1.05	1.15	1.21	0.04	0.50	0.35

performance of three different rib cases (45 deg, inverted 45 deg, and 90 deg) as well as smooth case was studied. Regionally averaged heat transfer distribution reported in this study can help designer determine the rib configuration for internal cooling channels. The experiments were conducted under high rotation number and high buoyancy parameter to simulate the actual engine condition. The results can be correlated with different density ratios, Reynolds numbers, and rotational speeds by rotation number and buoyancy parameter. Based on the results reported, the following conclusion can be drawn.

(1) L1 and T1 surfaces are the most critical regions near the leading edge of the turbine blade. In these two surfaces, staggered 45 deg rib has the highest heat transfer enhancement ($\mathrm{Nu}/\mathrm{Nu}_o$) and TP at stationary condition; while staggered 45 deg rib and 90 deg rib have the higher comparable heat transfer enhancement ($\mathrm{Nu}/\mathrm{Nu}_o$) at rotating condition.
(2) On the L2 and T2 surfaces, inverted 45 deg rib has the highest heat transfer and thermal performance at stationary condition; inverted 45 deg rib and 90 deg rib show comparable heat transfer at rotating condition.
(3) 90 deg rib shows the highest friction factor ratio; 45 deg angled rib and inverted 45 deg angled rib have similar friction factor ratio.
(4) Rotation has more profound effects on heat transfer enhancement for 90 deg rib and inverted 45 deg angled rib than the 45 deg angled rib.

Acknowledgment

This research project has been funded by Solar Turbines Inc.

Nomenclature

A = area of the copper plate
D_h = channel hydraulic diameter
e = rib height
f = friction factor
f_o = fully developed friction factor in nonrotating, smooth pipe
h = regionally averaged heat transfer coefficient
k = thermal conductivity of the coolant
L = length of the heated portion of the test section
L_e = length of the unheated portion of inlet part
Nu = regionally averaged Nusselt number
Nu_o = Nusselt number of the fully developed turbulent flow in nonrotating smooth tube
P = rib spacing
Pr = Prandtl number of the coolant
Q_{loss} = heat loss through the wall
Q_{in} = heat input at the wall
R_x = local radius of rotation
Re = Reynolds number, $\rho V D_h/\mu$
Ro = Rotation number, $\Omega D_h/V$
$T_{w,x}$ = local wall temperature
$T_{b,x}$ = local coolant bulk temperature
$T_{f,x}$ = local film temperature $(=(T_{w,x}+T_{b,x})/2)$
V = bulk velocity in streamwise direction
α = rib angle of attack
ρ = density of the coolant
$(\Delta\rho/\rho)_x$ = local coolant-to-wall density ratio $(=(T_{w,x}-T_{b,x})/T_{f,x})$
Ω = rotational speed

References

[1] Han, J. C., Dutta, S., and Ekkad, S. V., 2000, *Gas Turbine Heat Transfer and Cooling Technology*, Taylor & Francis, New York.
[2] Han, J. C., 1984, "Heat Transfer and Friction in Channels With Two Opposite Rib-Roughened Walls," ASME J. Heat Transfer, **106**, pp. 774–781.
[3] Han, J. C., 1988, "Heat Transfer and Friction Characteristics in Rectangular Channels With Rib Turbulators," ASME J. Heat Transfer, **110**, pp. 321–328.
[4] Han, J. C., and Zhang, P., 1991, "Effect of Rib-Angle Orientation on Local Mass Transfer Distribution in a Three-Pass Rib-Roughened Channel," ASME J. Turbomach., **113**, pp. 123–130.
[5] Park, J. S., Han, J. C., Huang, Y., and Ou, S., 1992, "Heat Transfer Performance Comparisons of Five Different Rectangular Channels With Parallel Angled Ribs," Int. J. Heat Mass Transfer, **35**(11), pp. 2891–2903.
[6] Lowdermilk, W. H., Weiland, W. F., and Livingood, J. N. B., 1954, "Measurement of Heat Transfer and Friction Coefficients for Flow of Air in Noncircular Ducts at High Surface Temperatures," NACA RM E53J07.
[7] Metzger, D. E., and Vedula, R. P., 1987, "Heat Transfer in Triangular Channels With Angled Roughness Ribs on Two Walls," Exp. Heat Transfer, **1**, pp. 31–44.
[8] Zhang, Y. M., Gu, W. Z., and Han, J. C., 1994, "Augmented Heat Transfer in Triangular Ducts With Full and Partial Ribbed Walls," J. Thermophys. Heat Transfer, **8**(3), pp. 574–579.
[9] Haasenritter, A., and Weigand, B., 2001, "Heat Transfer in Triangular Rib-Roughened Channels," ASME Paper No. NHTC 2001-20245.
[10] Ahn, S. W., and Son, K. P., 2002, "Heat Transfer and Pressure Drop in the Roughened Equilateral Triangular Duct," Int. Commun. Heat Mass Transfer, **29**, pp. 479–488.
[11] Amro, M., Weigand, B., Poser, R., and Schnieder, M., 2007, "An Experimental Investigation of the Heat Transfer in a Ribbed Triangular Cooling Channel," Int. J. Therm. Sci., **46**, pp. 491–500.
[12] Taslim, M. E., Li, T., and Spring, S. D., 1998, "Measurements of Heat Transfer Coefficients and Friction Factors in Passages Rib-Roughened on All Walls," ASME J. Turbomach., **120**, pp. 564–570.
[13] Takeishi, K., Kitamura, T., Matsuura, M., and Shimizu, K., 2003, "Heat Transfer Characteristic of a Triangular Channel With Turbulence Promoter," *Proceedings of the International Gas Turbine Congress*, Tokyo, Japan, Paper No. TS-080.
[14] Dutta, S., Han, J. C., and Lee, C. P., 1995, "Experimental Heat Transfer in a Rotating Triangular Duct: Effect of Model Orientation," ASME J. Heat Transfer, **117**, pp. 1058–1061.
[15] Lee, D. H., Rhee, D. H., and Cho, H. H., 2006, "Heat Transfer Measurements in a Rotating Equilateral Triangular Channel With Various Rib Arrangements," ASME Paper No. GT 2006-90973.
[16] Wagner, J. H., Johnson, B. V., and Hajek, T. J., 1991, "Heat Transfer in Rotating Passages With Smooth Walls and Radial Outward Flow," ASME J. Turbomach., **113**, pp. 42–51.
[17] Wagner, J. H., Johnson, B. V., and Kopper, F. C., 1991, "Heat Transfer in Rotating Serpentine Passages With Smooth Walls," ASME J. Turbomach., **113**, pp. 321–330.
[18] Johnson, B. V., Wagner, J. H., Steuber, G. D., and Yeh, F. C., 1994, "Heat Transfer in Rotating Serpentine Passages With Trips Skewed to the Flow," ASME J. Turbomach., **116**, pp. 113–123.
[19] Zhou, F., Lagrone, J., and Acharya, S., 2004, "Internal Cooling in 4:1 AR Passages at High Rotation Numbers," ASME Paper No. GT 2004-53501.
[20] Liou, T. M., Chang, S. W., Hung, J. H., and Chiou, S. F., 2007, "High Rotation Number Heat Transfer of 45° Rib-Roughened Rectangular Duct With Two Channel Orientations," Int. J. Heat Mass Transfer, **50**, pp. 4063–4078.
[21] Liu, Y. H., Huh, M., Han, J. C., and Chopra, S., 2008, "Heat Transfer in a Two-Pass Rectangular Channel ($AR=1:4$) Under High Rotation Numbers," ASME J. Heat Transfer, **130**(8), p. 081701.
[22] Wright, L. M., Liu, Y. H., Han, J.-C., and Chopra, S., 2008, "Heat Transfer in a Trailing Edge, Wedge-Shaped Cooling Channels Under High Rotation Numbers," ASME J. Heat Transfer, **130**(7), p. 071701.
[23] Liu, Y. H., Huh, M., Rhee, D. H., Han, J. C., and Moon, H. K., 2008, "Heat Transfer in Leading Edge, Triangular Shaped Cooling Channels With Angled Ribs Under High Rotation Numbers," ASME Paper No. GT-2008-50344.
[24] Kline, S. J., and McClintock, F. A., 1953, "Describing Uncertainty in Single-Sample Experiments," Mech. Eng. (Am. Soc. Mech. Eng.), **75**, pp. 3–8.